land

MDPI

Brief Report

Climatic Niche of Vegetation Greenness Is Likely to Be Conservative in Degraded Land

Guoqing Li * and Jinghua Huang

State Key Laboratory of Soil Erosion and Dryland Farming on the Loess Plateau, Institute of Soil and Water Conservation, Northwest A&F University, Xianyang 712100, China; jhhuang@nwsuaf.edu.cn
* Correspondence: liguoqing@nwsuaf.edu.cn; Tel.: +86-29-8701-2411

Abstract: Satellite data have been widely used to study changes in vegetation greenness in geographical space; however, this change is rarely considered in climatic space. Here, the climatic niche dynamics of vegetation greenness, represented by the normalized difference vegetation index (NDVI), was quantified in the climate space of the Loess Plateau, a piece of degraded land greening significantly from 2000 to 2018. The niche similarity test was used to examine the niche conservatism of vegetation greenness during the 19 years of restoration. The results show that the climate niche of vegetation greenness is always more similar than expected. The stability niche occupied most parts (83–98%) of their climatic niche, and niche overlap reached 0.52–0.69. Climate niche conservatism suggests that potential greenness constructed by statistical methods could be used as a criterion or baseline for ecosystem function restoration on the Loess Plateau. The study also suggests that the integrated niche similarity test in decision-making for restoration of degraded land will clarify our understanding of the climatic niche dynamics of vegetation greenness and the making of forecasts.

Keywords: vegetation greenness; environmental space; niche dynamics; niche dynamics; niche similarity test

check for updates

Citation: Li, G.; Huang, J. Climatic Niche of Vegetation Greenness Is Likely to Be Conservative in Degraded Land. *Land* **2022**, *11*, 894. https://doi.org/10.3390/land11060894

Academic Editor: Nir Krakauer

Received: 2 May 2022
Accepted: 10 June 2022
Published: 11 June 2022

Publisher's Note: MDPI stays neutral with regard to jurisdictional claims in published maps and institutional affiliations.

Copyright: © 2022 by the authors. Licensee MDPI, Basel, Switzerland. This article is an open access article distributed under the terms and conditions of the Creative Commons Attribution (CC BY) license (https://creativecommons.org/licenses/by/4.0/).

1. Introduction

The spatial and temporal variations of climate drives many ecological and evolutionary processes in the terrestrial ecosystem [1,2]. Long term climate change has been one of the main drivers of changes in biodiversity [3], vegetation growth [4], and the global carbon cycle [5]. Climate spatial variation determines vegetation zone distribution across the earth, as well as species distribution ranges [6–8].

Early ecologists have long recognized the role of climate in vegetation and put forward the mono-climax theory [6,7,9]. It is considered that the final state of vegetation in a place after long-term succession is completely controlled by climate. Based on this theory, many vegetation climate correlation models and mechanism models were used to simulate and predict potential vegetation, that is, to find the climatic climax state of vegetation [7,10,11]. The emergence of these models provides favorable tools to understand climax vegetation on our planet. With the accumulation of climate data from global climate stations, two very typical global climate data sets have sprung up: (1) the WorldClim [12]; (2) CRU TS datasets [13]. The application potential of these models also had extensive transfer capability.

These models can be used to inform vegetation management. However, the first factor we need to know about is the current state of vegetation. In the past, vegetation sampling using the quadrat method has been used to detect vegetation status [14–16]. This method consumes many human, material and financial resources. Although the vegetation quadrat data is being integrated at present (e.g., [17,18]), the integrated databases are still scattered in space and discontinuous in time scale.

The development of remote sensing technology has completely solved the difficulty in vegetation monitoring [19,20]. Vegetation parameters with continuous time and spatial scale can be obtained by using multi platforms (e.g., towers, drones, aircraft, and

satellites) [21], multi-sensor [22–24], as well as ground observation data. Multiple remote sensing data provide a large number of vegetation parameters, such as function, health, and structure [25]. Based on these parameters, many new methods of vegetation monitoring, assessment and management strategies have been developed under the guidance of ecological theory and models [26,27]. One of the important applications is the long-term change trends in vegetation greenness [28]. If the greenness has declined over a long time, it is considered that the vegetation is in a degraded state; if the greenness has improved over a long time, it is considered that the vegetation is in a state of restoration.

Climate factors and human factors are the two main driving factors in exploring the causes of vegetation greenness change (e.g., [29,30]). Two methods were usually used to separate their interaction: one is the residual method (e.g., [30]); the other is the baseline method (e.g., [31]). The residual method suggests that the residual of regression between vegetation greenness and climate represents the role of human beings. The baseline method suggests that the observed vegetation greenness deviates from the ideal state (deficiency or redundancy) and is considered to be the impact of human activities.

Both residual method and baseline method, in fact, directly or indirectly use a very important concept, namely "potential greenness of vegetation or potential vegetation greenness", although previous studies have not clearly defined this concept. We suggest that the concept is very close to the concept of mono-climax vegetation [9]. Therefore, potential vegetation greenness can be defined as the greenness state of mono-climax vegetation without human interference.

The concept of potential vegetation greenness has been widely used in the process of conservation, afforestation, and vegetation restoration in degraded land [32,33]. Applying these concepts, several niche models were constructed using statistical methods (e.g., regression, CART, ANN, MaxEnt, SVM, and random forest) based on observed occurrence (suitability) and climatic variables to characterize the climatic requirements of the target vegetation and species [31,34]. The common assumption for these models is that entity climatic niche should be conservative [35]. Nevertheless, the validity of this hypothesis requires testing before applying these models as conservation or restoration criteria (baseline).

More attention has been paid to climatic niche conservatism at the species level owing to the rapid development of niche theory [33] and tools [36,37]. For example, Soberon and Nakamura [35] developed a famous biotic, abiotic, and movements concept framework for understanding niche and distribution. Petitpierre et al. [38] reported a large-scale test of climatic niche conservatism for 50 invasive plant species and suggested that niche shifts are rare invasive plant species. Li et al. [39] suggested that black locust (*Robinia pseudoacacia*) conserves its climatic niche in the afforestation process worldwide.

However, statistical quantification of climatic niche conservatism of vegetation greenness has lagged in comparison [36,37] and is less focused. For example, Stoms and Hargrove [31] first developed a statistical method to estimate the potential normalized difference vegetation index (NDVI, a vegetation greenness indicator) as a baseline for monitoring ecosystem functioning. They recognized the importance of niche conservatism and suggested finding a suitable period for simulating rather than testing niche conservatism. However, they did not provide an objective method for determining the optimal period. Follow-up studies of potential vegetation greenness were a continuation of this pragmatic idea [40,41] but do not focus on hypothesis tests such as species potential distribution.

Using statistical niche models to study the potential distribution of species and vegetation greenness has a similar algorithm [31,33,34]. The niche and distribution theory should be fully applicable to the study of potential vegetation greenness to promote interdisciplinary integration. Currently, niche similarity and equivalency tests are the two most frequently used statistical methods for hypotheses of niche divergence or conservatism [36,37], indicating whether niches are different between species, ranges, or periods. A recent principal component method with kernel smoothing can visualize niche dimen-

sions [37]. An excellent framework could be used to gain insights into niche shift dynamics by combining these methods.

This study aimed to quantify the niche dynamics of vegetation greenness on degraded land during 19 years of restoration using niche similarity rather than niche equivalency tests. The equivalence test is considered strict; even if the alternative hypothesis is rejected, the similarity of niches cannot be denied [37]. Niche similarity testing is a relatively loose and comfortable test that has been successfully and widely used in research on ecology and evolution [38,39]. The results obtained will provide a theoretical basis for the application of the concept of potential vegetation greenness in ecological restoration and monitoring of degraded land.

2. Materials and Methods

2.1. Study Area

The Loess Plateau of Northwest China (33°43′–41°16′ N, 100°54′–114°33′ E) is a typical degraded region with a total area of approximately 6.5 × 10^5 km^2 (6.76% of the land area of China). It is a highland region with an average elevation of approximately 1200 m [42]. The annual mean temperature is 7.6 °C, while the annual precipitation is approximately 441 mm [43]. The complicated landscape, frequent droughts, severe soil erosion, and sustained deterioration of the ecosystem have made this region the subject of research worldwide.

Many ecological engineering projects have been implemented to improve ecosystem functions, such as the Three-North Shelterbelt Project, the Grain for Green Project, and a soil-retaining dam project [42]. A significant greening trend has been detected, and soil erosion rates are controlled on the plateau [44,45]. This provides a good object to test the niche conservation hypothesis of vegetation greenness in the climatic space of degraded land. The location of the Loess Plateau with NDVI images from 2000 and 2018 is provided in Figure 1.

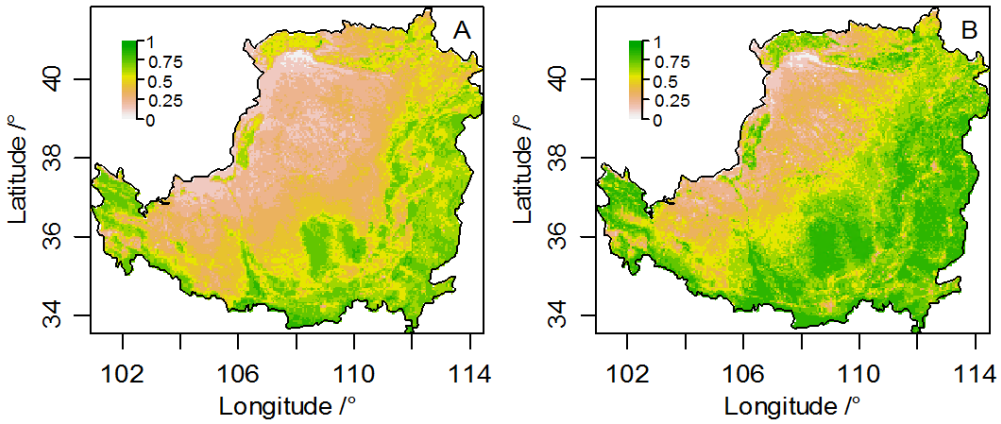


Figure 1. The location of the Loess Plateau with its maximum yearly NDVI image from 2000 (**A**) and 2018 (**B**).

2.2. Vegetation Greenness Data

Vegetation greenness is an index of vegetation function. Vegetation greenness has been used as a proxy for above ground biomass, the carbon and water cycles, energy flows, and other terrestrial ecosystem processes [46]. Currently, more than 100 indices have been developed to describe vegetation greenness (see review in [47]), such as normalized difference vegetation index (NDVI), ratio vegetation index, difference vegetation index, atmospherically resistant vegetation index, and adjusted-soil vegetation index. Here, we selected NDVI for vegetation greenness as model input due to its extensive use and data availability.

NDVI is often used to characterize the trend of greening or browning of vegetation and to reflect the adaptation of vegetation to climate change [48,49]. It is the ratio of the

difference and sum of the reflectivity of the near-infrared band with the red band. Here, continuous annual series of NDVI satellite remote sensing data were obtained from the Resource and Environment Science and Data Center (RESDC, doi:10.12078/2018060601) [50]. These NDVI datasets were generated using the maximum synthesis method in a year time frame from 1998 to 2018 (grid cell size of 1000 m × 1000 m with a Clark reference system 1866), thus including 21 layers. These have been widely used to monitor vegetation changes in China [41,44,48].

2.3. Climate Variables

Availability of climatic layers representing climatic conditions across the study area is essential. Among the various sources of climate data, the Worldclim database has represented a breakthrough, as it has provided ecological modelers with worldwide climate surfaces at various grid resolutions for current conditions as well as for past and future time horizons [51]. Monthly climate data (minimum temperature, maximum temperature, and precipitation) were obtained from the WorldClim 2.1 version database (http://www.worldclim.org, accessed on 2 March 2021) [12] for 1998–2018 at a global scale (grid cell size of 2.5′ × 2.5′ with WGS84 reference system). Then, 19 bioclimatic variables on the annual scale were calculated based on the three climatic variables [12], which have clearer biological significance than variables on a monthly scale. The 19 bioclimatic variables are shown in Table 1.

Table 1. Bioclimatic variables used in this study.

Climatic Variables	Abbreviation	Unit
Annual mean temperature	Bio1	°C
Mean diurnal range (mean of monthly (max temp-min temp))	Bio2	°C
Isothermality (Bio2/Bio7) (×100)	Bio3	/
Temperature seasonality (standard deviation ×100)	Bio4	°C
Max temperature of warmest month	Bio5	°C
Min temperature of coldest month	Bio6	°C
Temperature annual range (Bio5–Bio6)	Bio7	°C
Mean temperature of wettest quarter	Bio8	°C
Mean temperature of driest quarter	Bio9	°C
Mean temperature of warmest quarter	Bio10	°C
Mean temperature of coldest quarter	Bio11	°C
Annual precipitation	Bio12	mm
Precipitation of wettest month	Bio13	mm
Precipitation of driest month	Bio14	mm
Precipitation seasonality (coefficient of variation)	Bio15	%
Precipitation of wettest quarter	Bio16	mm
Precipitation of driest quarter	Bio17	mm
Precipitation of warmest quarter	Bio18	mm
Precipitation of coldest quarter	Bio19	mm

2.4. Experiment Design and Statistical Analysis

2.4.1. Data Preprocessing and Preparation

Climate determines the pattern and process of vegetation on a large scale and coarse grain size. Therefore, in order to match the scale of the scientific problems studied, all raw data collected and generated were resampled by kriging interpolation to a spatial resolution of 7.5′ × 7.5′ with the WGS84 reference system. This resolution was assumed to be sufficient to reflect the impact of climate on vegetation pattern and climatic process in the region. The reason for selection of kriging interpolation was that the method has good efficiency for data with spatial autocorrelation. All NDVI data and climatic layers were masked on the Loess Plateau. Through such standardization processes, a total of 4234 grid cells on the Loess Plateau are our research target areas.

To cover up the influence of random factors, the average of the maximum NDVI value in 1998, 1999, and 2000 was used to represent the greenness state in 2000, and the average of

the maximum NDVI value in 2016, 2017, and 2018 was used to represent the greenness state in 2018. The niche dynamics of vegetation greenness were tested and analyzed between the two NDVI datasets.

The niche similarity test requires occurrence or presence data [37]. The NDVI value was a continuous numerical type. Therefore, it is necessary to divide the NDVI into binary data types to meet detection needs. To obtain full information of continuous data, we set 4 NDVI threshold scenarios with equal intervals of 0.2, including 0.15, 0.35, 0.55, and 0.75.

There should be 4 pairs of binary layers (coded as 0 and 1), in which 1 represents greenness higher than the specific threshold, and 0 represents greenness lower than the specified threshold. We randomly selected 100 points without replacing code equal to 1 in 2000 and 2018 binary maps for every pair of binary layers separately. These points represent the climatic niche of vegetation greenness during the two time periods.

2.4.2. Statistical Test of Niche Dynamics, Niche Overlap and Visualization

Statistical analysis of niche dynamics was performed using the niche similarity test in the ecospat packages in the R platform [52], which is based on a principal component analysis (PCA) approach and a kernel smoothing method. The method involved six steps:

(1) Reduction multiple climate variables into two axes using PCA method

The reason to use only two axes was that increased dimensionality brings greater challenges in terms of interpretation, visualization and additional technical aspects. Thus, the first two axes constitute the climate space for the study region.

(2) Calculation of the density of occurrences and climate along two PCA axes

The climate space was divided into a grid of 100 × 100 cells. Occurrence records were plotted on the gridded climatic space with 100 × 100 dimensions. Each cell corresponds to a unique climatic condition present at one or more sites in geographical space. A kernel smoothing method was used to calculate the density of occurrences, as well as climate density. Then, a relative abundance index was calculated as follows:

$$o_{ij} = \frac{ds_{ij}}{\max(ds)} \quad (1)$$

where ds_{ij} is the kernel density estimation of occurrence in a grid cell, max(ds) is the maximum kernel density in any one cell, and O_{ij} is a relative abundance index.

In a similar manner, the smoothed density of available climate c_{ij} was calculated as follows:

$$c_{ij} = \frac{dc_{ij}}{\max(dc)} \quad (2)$$

where dc_{ij} is the number of sites with environment v_{ij} and max(dc_{ij}) is the number of cells with the most common environment in the study area.

(3) Calculation of unbiased occurrence densities

The unbiased occurrence densities (z_{ij}) were calculated as follows:

$$z_{ij} = \frac{ds_{ij}/dc_{ij}}{\max(ds/dc)} \quad (if e_{ij} \neq 0) \quad (3)$$

and

$$z_{ij} = 0 \quad if \quad e_{ij} = 0 \quad (4)$$

where z_{ij} ranges between 0 and 1 and ensures a direct and unbiased comparison of occurrence densities between different entities occurring in ranges where environments are not equally available.

(4) Measurement of niche overlap along two PCA axes

Niche overlap was calculated using a well-established Schoener's D metric [53], which ranges from 0 (no overlap) to 1 (complete overlap). An unbiased estimation of D was calculated using a kernel density function applied to the occurrence densities and environment density. It was calculated as follows:

$$D = 1 - \frac{1}{2}\left(\sum_{ij}|z_{1ij} - z_{2ij}|\right) \quad (5)$$

where z_{1ij} is entity 1 occupancy and z_{2ij} is entity 2 occupancy. This metric varies between 0 (no overlap) and 1 (complete overlap).

Following Petitplerre et al. [38], three categories of niche dynamics (Climatic niche partitioning, Figure 2) were calculated as follows: niche stability, i.e., the proportion of the densities in 2000 that overlap with 2018; niche unfilling, i.e., the proportion of the densities in 2000 that do not overlap with 2018; niche expansion, i.e., the proportion of the densities in 2018 that do not overlap with 2000 (or 1-stability).

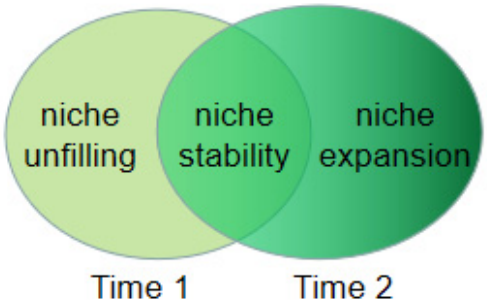


Figure 2. Climatic niche partitioning between time 1 to time 2.

(5) Statistical tests of niche similarity

The niche similarity test addresses whether the environmental niche occupied in one range is more similar to the one occupied in the other range than would be expected by chance. For this test, we randomly shifted the entire observed density of occurrences in one range (the center of the simulated density of occurrence was randomly picked among available environments) and calculated the overlap of the simulated niche with the observed niche in the other range.

This procedure was repeated 100 times to generate a null distribution of the Schoener's D metric, which ranges from 0 (no overlap) to 1 (complete overlap), to determine the statistical significance. If the observed D and values are greater than 95% of the simulated values, this indicates that climatic niches are more similar than random. If it is less than 95% of the simulated values, it indicates climatic niche divergence. The niche similarity test determined whether the climatic niche of vegetation greenness in the year 2000 was better at predicting that in 2018 than randomly generated niches from a background region.

(6) Occurrence densities in climatic niche space were mapped using PCA to visualize the dynamics of niche centroid and breadth of the two dimensions between the two time periods.

3. Results

3.1. Change in Vegetation Greenness

The NDVI change on the Loess Plateau from 2000 to 2018 is shown in Figure 3, which demonstrates that the vegetation greenness in this area has increased significantly. The average maximum yearly NDVI value increased from 0.47 in 2000 to 0.6 in 2018 on the plateau. This shows that the vegetation greenness has increased by 27.7%. The increase of greenness is mainly located in the middle of the Loess Plateau.

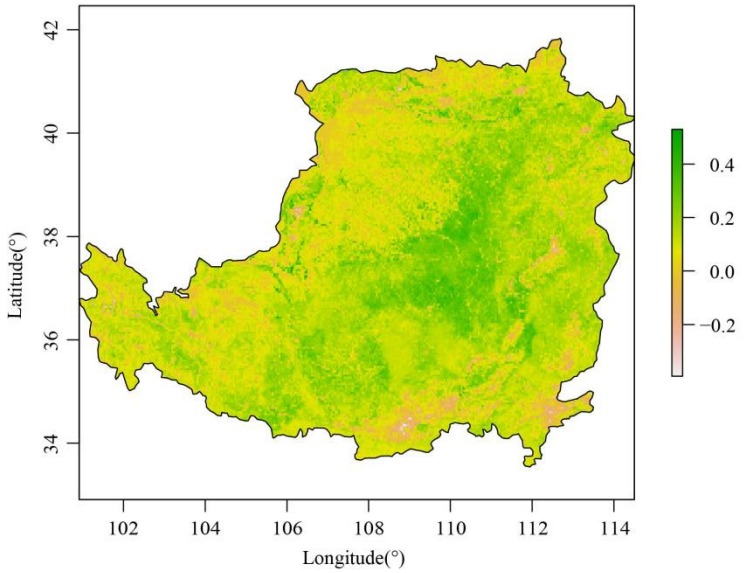


Figure 3. The maximum yearly NDVI change on the Loess Plateau from 2000 to 2018.

3.2. Climatic Niche Dimensions

The correlation circle map and coefficients of the 19 bioclimatic variables are shown in Figure 4 and Table A1. The first two PCA axes accounted for 75.42% of the variation in the data (PCA1: 45.92%; PCA2: 25.5%). The first PCA axis is dominated by a heat-water gradient from warm and wet conditions to dry and cold conditions during coldest month (January), coldest driest quarter (January, February, December) (high correlation variables including min temperature of coldest month (Bio6), mean temperature of driest quarter (Bio9), mean temperature of coldest quarter (Bio11), annual precipitation (Bio12), precipitation of driest quarter (Bio17)), whereas the second axis predominantly represents the heat condition during the warmest month (August) and warmest quarter (July, August, September) (high correlation variables including max temperature of warmest month (Bio5), mean temperature of warmest quarter (Bio10)).

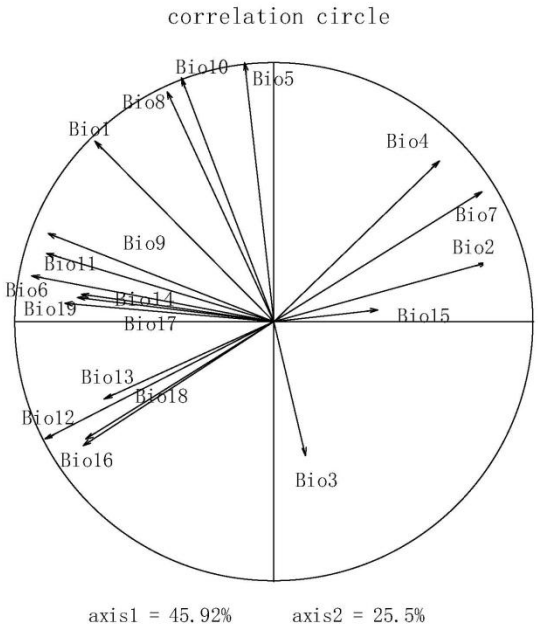


Figure 4. Correlation circle map of principal component analysis (PCA) for 19 bioclimatic variables. Coefficients of the 19 bioclimatic variables are shown in Table A1.

3.3. Climatic Niche Visualization

Niche visualization of vegetation greenness between 2000 and 2018 was carried out in a gridded climatic space formed by the first two axes of PCA based on 19 climatic variables (Figure 5). The results show that the centroid shift of background climate of the Loess Plateau mainly migrates along the first axis from right to left with a warmer and wetter condition from 2000 to 2018 (the red dashed arrows), whereas that of vegetation greenness niche shows a different shift pattern under different NDVI classification (the red solid arrows). The higher the NDVI classification, the more inconsistent the shift direction with the background climatic conditions. This indicates that non-climatic factors are likely to be driving the change of the niche of this vegetation level, such as vegetation growth (biological factors) or human factors.

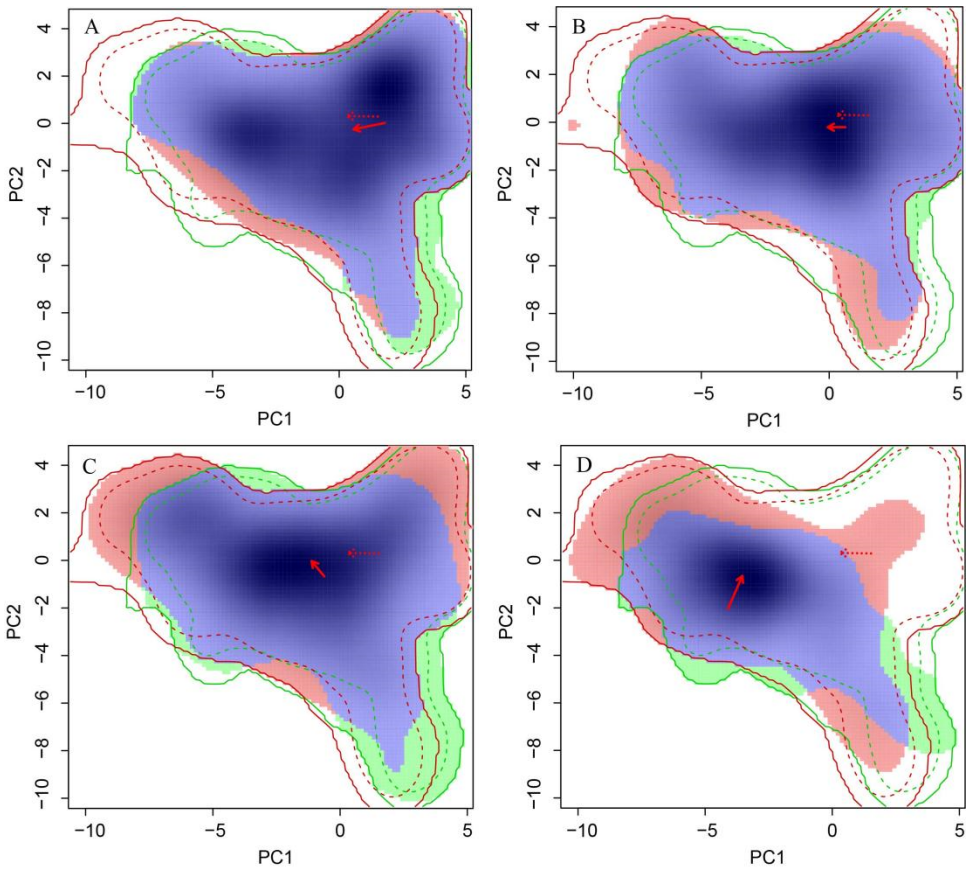


Figure 5. Niche dynamics of vegetation greenness. (**A**) NDVI greater than 0.15; (**B**) NDVI greater than 0.35; (**C**) NDVI greater than 0.55; (**D**) NDVI greater than 0.75. Solid and dashed lines represent 100% and 75% of background climate niche (study region) in 2000 and 2018, separately. Green represents climate niche in the year 2000 for corresponding NDVI classification; blue indicates climate niche shared by two years 2000 and 2018 for corresponding NDVI classification; red represents climate niche in the year 2018 for corresponding NDVI classification. Shading density indicates occurrence density of NDVI classification in the year 2018. The red solid arrows and dashed arrows show the centroid shift in climate space between two periods for corresponding NDVI classification and background region.

The niche overlap of vegetation greenness between 2000 and 2018 was mainly in the range of 0.52–0.66. Climatic niche centroids and breadth visualization suggested that the niche of vegetation greenness is stable during the greening process on the Loess Plateau. However, we do not know whether the niche of vegetation is conservative or not. In the statistical sense, has the niche changed? This requires a similarity test to answer the question.

3.4. Climatic Niche Similarity Test

The niche similarity tests were carried out in these four scenarios separately, and the test results are shown in Figure 6. The results show that the climate niche of vegetation greenness is always more similar than expected by chance (100 permutations test $p < 0.05$). The findings indicate that the climatic niche of vegetation greenness is conservative during the greening process on the Loess Plateau.

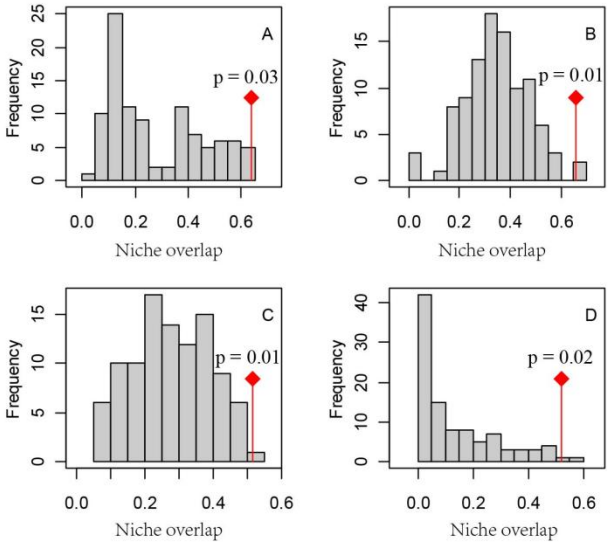


Figure 6. Niche similarity test of vegetation greenness. (**A**) NDVI greater than 0.15; (**B**) NDVI greater than 0.35; (**C**) NDVI greater than 0.55; (**D**) NDVI greater than 0.75. Bars represent the frequency of niche overlap D value. Red line diamond-shaped point represents observed niche overlap D value. *p* value represents the significant test.

3.5. Climatic Niche Stability, Expansion, and Unfilling

Climatic niche partitioning showed that the stability niche occupied a proportion of 83–98% of their climatic niches, and the expansion niche occupied the proportion of 3–17% of their climatic niche (novel habitat, Table 2). There are no or very few unfilling climatic niches (1–9%). It appears that the climatic niche of vegetation greenness is stable and conservative during the greening process on the Loess Plateau.

Table 2. Climatic niche stability, expansion, and unfilling and niche overlap of vegetation greenness.

	NDVI Threshold	Niche Expansion	Niche Stability	Niche Unfilling	Niche Overlap
1	0.15	0.03	0.97	0.03	0.64
2	0.35	0.04	0.96	0.01	0.66
3	0.55	0.07	0.93	0.07	0.52
4	0.75	0.17	0.83	0.09	0.52

4. Discussion

4.1. Niche Dynamics and Interpretation

Vegetation and greenness in the Loess Plateau were seriously degraded [41,42]. Since the implementation of various restoration projects in 1999, the average NDVI greenness of vegetation increased from 0.47 in 2000 to 0.6 in 2018 on the plateau. The increase of greenness is mainly located in the middle of the Loess Plateau. The vegetation greening pattern we obtained is very similar to many studies on the change of vegetation greenness on the Loess Plateau [54–56]. The main reason is that these studies all use a similar vegetation index to describe the greenness of vegetation.

In explaining the reason for vegetation greening, Xin et al. [54] believed that precipitation change was an important cause of vegetation change, human activities were

the cause of vegetation degradation in humid areas, and irrigation agriculture was the cause of vegetation greening in arid areas. Zhang et al. [55] suggested that climate change was the dominant factor in vegetation greening, but urbanization had led to vegetation degradation in some areas of the Loess Plateau. Chang and Xie [56] separated the relative importance of the two factors by using the residual method and they suggested that the climate contribution rate to vegetation greenness change on the Loess Plateau was 77%, and that the contribution rate of human activities was 23%.

In contrast, national and global scale studies suggested that the role of human activities was considered to be the leading factor in vegetation greening. For example, Liu and Gong [57] showed that the vegetation greening in Shaanxi and Shanxi (belonging to the Loess Plateau) had increased significantly, but the driving effect of climate change was not large. Chen et al. [58] thought that China's greening was mainly caused by afforestation projects.

Whether the geographical pattern of vegetation greening is dominated by climate or human interference factors, it is an indisputable fact that the geographical pattern of vegetation greening can be easily captured by remote sensing images. However, this observation cannot reflect the dynamics of vegetation greenness in climate space. Will vegetation greenness increase (shift) in geographical space lead to changes in climatic space? In other words, is vegetation greenness conservative in climate space? The answer to these questions is of great significance for understanding vegetation dynamics and the ecological evolution of vegetation greenness. In order to solve this problem, this study attempts to map different levels of greenness in geographical distribution space to the corresponding climate space, and test niche centroid dynamics in climate space.

Our niche similarity test showed that the climatic niche of vegetation greenness was always conservative under any NDVI threshold scenario in the period. The niche overlap of vegetation greenness is larger (0.52–0.69) than similar studies on species for introduction or invasion scenarios [38,39]. Additionally, the stability niche occupied 83–98% of their climatic niche in 2018. This indicates that the vegetation greenness of different greenness grades in the Loess Plateau tends to remain constant and conservative, and the climatic niche of vegetation greenness does not change significantly with the shift in geographical and spatial niche.

It is likely that the vegetation on the Loess Plateau which has been degraded in the past, caused by both climate change and human activities, did not change the centroid of climatic niche space of vegetation greenness. During the decades of greenness restoration of vegetation after returning farmland to forest, the climate niche has always remained stable. This seems different from range shift pattern results based on geospatial analysis of greenness on the Loess Plateau [41,42,44,54–56]. This suggest that vegetation greenness on the Loess Plateau has migrated to the north by tens to hundreds of kilometers. We believe that the similarity test of niche centroid shift of greenness in climatic space is not contradictory to the observation of spatial niche centroid shift in geographical space. Both can complement each other. For example, the divergence of NDVI in geographical space reflects the deficiency or redundancy of vegetation. The increase of vegetation greenness on the Loess Plateau was likely to have been a restoration of vegetation deficiency. The driving force of the increase was vegetation growth induced by climate.

The shift of vegetation greenness in geographical space reflects that vegetation pursues the constancy of climate niche, which means that vegetation greenness develops towards potential vegetation greenness, as well as an ideal state indicated by the climate climax theory [6,7,9,10]. Although there were strong human disturbances (such as cities, farmland, etc.) in some regions in the geographical space, which inhibit vegetation restoration, we believe that, once these interference factors are removed, the natural resilience of vegetation on the Loess Plateau will be quickly reflected by vegetation greening.

Although there were many agricultural or forestry activities, human disturbance has not broken the conservative law of vegetation green niche. Thus, the selection of an appropriate baseline will help to provide a reference system and formulate reasonable

vegetation management strategies according to the principle of similarity in climate space. This management experience can be similar to species level research [38,39]. For example, in the process of management and control of invasive species, according to the climate niche of the original area of invasive species, we can speculate on the possible geographical space of the possible invasion area, and then take preventive measures for the possible invasion area. In other words, it is effective and reasonable to use the concept of potential greenness as a guide for vegetation restoration in the Loess Plateau, that is, to use a niche model, as well as greenness data and climatic variables, to establish potential greenness, which can be used as a criterion and baseline for ecosystem function restoration [31,32]. Therefore, an integrated niche similarity test in decision-making will clarify our understanding of the climatic niche dynamics of vegetation greenness and the making of forecasts.

4.2. Limitations and Future Development

A niche similarity test was used to detect the niche centroid shift in this study. The data required for the method are occurrence data [37], whereas vegetation greenness data are in a continuous value format. The continuous value should be transformed into a binary structure under different thresholds to meet the requirements of the niche similarity test, which should cause a loss of useful information. Interestingly, the climatic niche dynamics of vegetation greenness are not sensitive to threshold selection on the Loess Plateau, showing a conservative niche of greenness vegetation. Nevertheless, the continuous characteristics of remote sensing data contain much more information than the binary structure of NDVI data. We suggest that the classification based on land use type or vegetation type or even species type may better reflect the process and mechanism of niche dynamics for these entities than that only based on the threshold NDVI value. Developing a unique niche similarity test method for remote sensing data should be the direction of future efforts.

Besides, range and grain size also need our significant attention, as they are at the core of the successful use of remote sensing data [59,60]. Range and grain size applied by a user normally involves the question: can he/she identify what he/she needs to identify on the remote sensing imagery [61]? In the context of detecting climate niche for vegetation greenness, it is generally believed that climate effect on vegetation should be at a large scale, and the corresponding grain size should be coarse, so as to capture the main role of climate dominance [33,34]. At the same time, it should be pay special attention to the accuracy of the climate data layer. We know that there are two main sources of public climate data [12,13], both of which are rough in resolution. This is far from matching with the high-resolution direction of remote sensing [62]. For example, Gong et al. [63] completed the global land cover map with 30 m resolution and then released a global land cover data with 10 m resolution [64]. Therefore, it is worth exploring whether the range size (study region) and grid size will affect the stability of the niche similarity test results.

Our case study shows that the vegetation greenness niche is conservative on the Loess Plateau. However, if the non-conservative niche occurs, how do we explain this? We suggest that this situation indicates that the climatic niche of vegetation greenness should be far away from the state of climatic climax, and the vegetation greenness should be dominated by non-climate factors, such as land clearing, deforestation, irrigation or fire. Non climatic factors have destroyed the climate niche space of the vegetation. Vegetation should be almost cleared for intensity management in geographical space. This situation is most likely to occur in areas of small- and medium-size or those dominated by human activities. In this case, vegetation greenness cannot be used as the baseline for vegetation restoration. We need enlarge the range of the study area and it is better to include natural vegetation or nature reserves. Only when the climate niche of vegetation greenness is conservative can it be used as the baseline for vegetation restoration.

The long-term accumulation of remote sensing data has allowed the exploration of spatiotemporal variations in vegetation greenness [58,65]. However, previous studies had widely monitored changes in vegetation greenness in geographical space [49,66], but they

rarely explored the changes in vegetation greenness in ecological or climatic space. Whether vegetation greenness is conservative in ecological space is of great significance in guiding the concept of potential vegetation greenness in the practice of ecosystem restoration. To the best of our knowledge, this is the first study to explore the niche dynamics of vegetation greenness in climate space using remote sensing data from degraded land. The theory and methods of niche conservatism tests are at the forefront in the field of ecology and evolution, and there are many outstanding methods, such as niche similarity tests, niche equivalence tests, niche centroid shift tests, and niche breadth shift tests [36,37,67]. There is great application potential for using this knowledge to analyze remote sensing data for the integration of interdisciplinarity.

5. Conclusions

Climatic niche dynamics of vegetation greenness were explored in climate space using remote sensing data on the Loess Plateau. The climatic niche of vegetation greenness is always conservative during vegetation greening in the Loess Plateau. Potential greenness constructed by statistical methods should be used as a criterion and baseline for ecosystem function restoration on the Loess Plateau. The integrated niche similarity test when decision-making for restoration of degraded land will clarify our understanding of the climatic niche dynamics of vegetation greenness and the making of forecasts.

Author Contributions: Conceptualization, G.L. and J.H.; methodology, G.L.; software, G.L.; validation, G.L. and J.H.; writing—original draft preparation, G.L.; writing—review and editing, G.L. and J.H.; project administration, G.L.; funding acquisition, G.L. and J.H. All authors have read and agreed to the published version of the manuscript.

Funding: This research was funded by the National Natural Science Foundation of China, grant number 31971488 and 31500449.

Institutional Review Board Statement: Not applicable.

Informed Consent Statement: Not applicable.

Data Availability Statement: Not applicable.

Acknowledgments: We are very grateful to academic editor and English editor for their valuable suggestions and language polishing, which significantly improved the manuscript. We thank WorldClim database and Resource and Environment Science and Data Center, China for their publicly available of climatic layers and remote sensing NDVI data.

Conflicts of Interest: The authors declare no conflict of interest.

Appendix A

Table A1. The relative importance of each of climatic factor on the first two PCA axes. The first PCA axis is dominated by the heat-water gradient from warm and wet conditions to dry and cold conditions, whereas the second axis predominantly represents the heat condition in the growth season.

Variable	PCA1	PCA2
Bio1	−0.68	0.68
Bio2	0.80	0.22
Bio3	0.12	−0.50
Bio4	0.62	0.61
Bio5	−0.11	0.98
Bio6	−0.91	0.17
Bio7	0.78	0.49
Bio8	−0.40	0.87
Bio9	−0.85	0.33

Table A1. *Cont.*

Variable	PCA1	PCA2
Bio10	−0.35	0.92
Bio11	−0.86	0.26
Bio12	−0.86	−0.44
Bio13	−0.64	−0.29
Bio14	−0.73	0.11
Bio15	0.39	0.05
Bio16	−0.72	−0.46
Bio17	−0.79	0.07
Bio18	−0.71	−0.44
Bio19	−0.74	0.09

References

1. Parmesan, G. Ecological and evolutionary responses to recent climate change. *Annu. Rev. Ecol. Evol. Syst.* **2006**, *37*, 637–669. [CrossRef]
2. Loarie, S.R.; Duffy, P.B.; Hamilton, H.; Asner, G.P.; Field, C.B.; Ackerly, D.D. The velocity of climate change. *Nature* **2009**, *462*, 1052–1055. [CrossRef] [PubMed]
3. Garcia, R.A.; Cabeza, M.; Rahbek, C.; Araujo, M.B. Multiple dimensions of climate change and their implications for biodiversity. *Science* **2014**, *344*, 1247579. [CrossRef] [PubMed]
4. Zhang, R.; Ouyang, Z.T.; Xie, X.; Guo, H.Q.; Tan, D.Y.; Xiao, X.M.; Qi, J.G.; Zhao, B. Impact of climate change on vegetation growth in arid northwest of China from 1982 to 2011. *Remote Sens.* **2016**, *8*, 364. [CrossRef]
5. Dixon, R.K.; Turner, D.P. The global carbon cycle and climate change: Responses and feedbacks from below-ground systems. *Environ. Pollut.* **1991**, *73*, 245–262. [CrossRef]
6. Woodward, F.I.; Lomas, M.R.; Kelly, C.K. Global climate and the distribution of plant biomes. *Philos. Trans. R. Soc. B* **2004**, *359*, 1465–1476. [CrossRef]
7. Holdridge, L.R. Determination of world plant formations from simple climate data. *Science* **1947**, *105*, 367–368. [CrossRef]
8. Solomou, A.; Proutsos, N.; Karetsos, G.; Tsagari, C. Effects of climate change on vegetation in Mediterranean forests: A review. *Int. J. Environ. Agric. Biotechnol.* **2017**, *2*, 240–247. [CrossRef]
9. Clements, F.E. Nature and Structure of the Climax. *J. Ecol.* **1936**, *24*, 252–284. [CrossRef]
10. Fang, J.Y. *Global Ecology and Ecological Response*; Higher Education Press: Beijing, China, 2001.
11. Hardtle, W. On the theoretical concept of the potential natural vegetation and proposals for an up-to-date modification. *Folia Geobot Phytotax* **1995**, *30*, 263–276. [CrossRef]
12. Hijmans, R.J.; Cameron, S.E.; Parra, J.L.; Jones, P.G.; Jarvis, A. Very high resolution interpolated climate surfaces for global land areas. *Int. J. Clim.* **2005**, *25*, 1965–1978. [CrossRef]
13. Harris, I.; Jones, P.D.; Osborn, T.J.; Lister, D.H. Updated high resolution grids of monthly climatic observations—The CRU TS3.10 Dataset. *Int. J. Clim.* **2014**, *34*, 623–642. [CrossRef]
14. Wiser, S.K. Achievements and challenges in the integration, reuse and synthesis of vegetation plot data. *J. Veg. Sci.* **2016**, *27*, 868–879. [CrossRef]
15. Kuhl, H.S.; Bowler, D.E.; Bosch, L.; Bruelheide, H.; Dauber, J.; Eichenberg, D.; Eisenhauer, N.; Fernandez, N.; Guerra, C.A.; Henle, K.; et al. Effective biodiversity monitoring needs a culture of integration. *One Earth* **2020**, *3*, 462–474. [CrossRef]
16. Aubin, I.; Cardou, F.; Boisvert-Marsh, L.; Garnier, E.; Strukelj, M.; Munson, A.D. Managing data locally to answer questions globally: The role of collaborative science in ecology. *J. Veg. Sci.* **2020**, *31*, 509–517. [CrossRef]
17. Dengler, J.; Jansen, F.; Glockler, F.; Peet, R.K.; De Caceres, M.; Chytry, M.; Ewald, J.; Oldeland, J.; Lopez-Gonzalez, G.; Finckh, M.; et al. The global index of vegetation-plot databases (GIVD): A new resource for vegetation science. *J. Veg. Sci.* **2011**, *22*, 582–597. [CrossRef]
18. Sabatini, F.M.; Lenoir, J.; Hattab, T.; Arnst, E.A.; Chytry, M.; Dengler, J.; Ruffray, P.D.; Hennekens, S.M.; Jandt, U.; Jansen, F.; et al. sPlotOpen—An environmentally balanced, open-access, global dataset of vegetation plots. *Glob. Ecol. Biogeogr.* **2021**, *30*, 1740–1764. [CrossRef]
19. Kerr, J.T.; Ostrovsky, M. From space to species: Ecological applications for remote sensing. *Trends Ecol. Evol.* **2003**, *16*, 299–305. [CrossRef]
20. Franklin, J.; Serra-Diaz, J.M.; Syphard, A.D.; Regan, H.M. Big data for forecasting the impacts of global change on plant communities. *Glob. Ecol. Biogeogr.* **2017**, *26*, 6–17. [CrossRef]
21. Toth, C.; Jozkow, G. Remote sensing platforms and sensors: A survey. *ISPRS J. Photogramm. Remote Sens.* **2016**, *115*, 22–36. [CrossRef]
22. Blais, F. Review of 20 years of range sensor development. *J. Electron. Imaging* **2004**, *13*, 231–240. [CrossRef]
23. Melesse, A.M.; Weng, Q.; Thenkabail, P.S.; Senay, G.B. Remote sensing sensors and applications in environmental resources mapping and modelling. *Sensors* **2007**, *7*, 3209–3241. [CrossRef] [PubMed]

24. Wang, J.; Gao, K.; Zhang, Z.; Ni, C.; Hu, Z.; Chen, D.; Wu, Q. Multisensor remote sensing imagery super-resolution with conditional GAN. *J. Remote Sens.* **2021**, *2021*, 9829706. [CrossRef]
25. Leitao, P.J.; Santos, M.J. Improving models of species ecological niches: A remote sensing overview. *Front. Ecol. Evol.* **2019**, *7*, 9. [CrossRef]
26. Xu, Y.; Yang, J.; Chen, Y. NDVI-based vegetation responses to climate change in an arid area of China. *Theor. Appl. Climatol.* **2016**, *126*, 213–222. [CrossRef]
27. Cavender-Bares, J.; Schneider, F.D.; Santos, M.J.; Armstrong, A.; Carnaval, A.; Dahlin, K.M.; Fatoyinbo, L.; Hurtt, G.C.; Schimel, D.; Townsend, P.A.; et al. Integrating remote sensing with ecology and evolution to advance biodiversity conservation. *Nat. Ecol. Evol.* **2022**, *6*, 506–519. [CrossRef]
28. Pan, N.; Feng, X.; Fu, B.; Wang, S.; Ji, F.; Pan, S. Increasing global vegetation browning hidden in overall vegetation greening: Insights from time-varying trends. *Remote Sens. Environ.* **2018**, *214*, 59–72. [CrossRef]
29. Jiang, L.; Jiapaer, G.; Bao, A.; Guo, H.; Ndayisaba, F. Vegetation dynamics and responses to climate change and human activities in Central Asia. *Sci. Total Environ.* **2017**, *599*, 967–980. [CrossRef]
30. Li, A.; Wu, J.; Huang, J. Distinguishing between human-induced and climate-driven vegetation changes: A critical application of RESTREND in Inner Mongolia. *Landsc. Ecol.* **2012**, *27*, 969–982. [CrossRef]
31. Stoms, D.; Hargrove, W. Potential NDVI as a baseline for monitoring ecosystem functioning. *Int. J. Remote Sens.* **2000**, *21*, 401–407. [CrossRef]
32. Boer, M.M.; Puigdefabregas, J. Predicting potential vegetation index values as a reference for the assessment and monitoring of dryland condition. *Int. J. Remote Sens.* **2003**, *24*, 1135–1141. [CrossRef]
33. Peterson, A.T.; Soberon, J.; Pearson, R.G.; Andersen, R.P.; Martinez-Meyer, E.; Nakamura, M.; Araujo, M.B. *Ecological Niches and Geographic Distributions*; Monographs in Population Biology No. 49; Princeton University Press: Princeton, NJ, USA, 2011.
34. Franklin, J. *Mapping Species Distributions: Spatial Interence and Prediction*; Cambridge University Press: Cambridge, UK, 2009.
35. Soberon, J.; Nakamura, M. Niches and distributional area: Concepts, methods, and assumptions. *Proc. Natl. Acad. Sci. USA* **2009**, *106*, 19644–19650. [CrossRef] [PubMed]
36. Warren, D.L.; Glor, R.E.; Turelli, M. Environmental niche equivalency versus conservatism: Quantitative approaches to niche evolution. *Evolution* **2008**, *62*, 2868–2883. [CrossRef] [PubMed]
37. Broennimann, Q.; Fitzpatrick, M.C.; Pearman, P.B.; Petitpierre, B.; Pellissier, L.; Yoccoz, N.G.; Thuiller, W.; Fortin, M.J.; Randin, C.; Zimmermann, N.E.; et al. Measuring ecological niche overlap from occurrence and spatial environmental data. *Glob. Ecol. Biogeogr.* **2012**, *21*, 481–497. [CrossRef]
38. Petitpierre, B.; Kueffer, C.; Broennimann, O.; Randin, C.; Daehler, C.; Guisan, A. Climatic niche shifts are rare among terrestrial plant invaders. *Science* **2012**, *335*, 1344–1348. [CrossRef] [PubMed]
39. Li, G.Q.; Zhang, X.Q.; Huang, J.H.; Wen, Z.M.; Du, S. Afforestation and climatic niche dynamics of black locust (Robinia pseudoacacia). *For. Ecol. Manag.* **2018**, *407*, 184–190. [CrossRef]
40. Xu, B.C.; Pan, J.H. Estimation of potential ecological carrying capacity in China. *Environ. Sci. Pollut. Res.* **2020**, *27*, 18044–18063. [CrossRef]
41. Suo, A.N.; Xiong, Y.; Xiong, Y.C.; Ge, J.P. Redundancy and deficiency of vegetaion in a typical region of the Loess Plateau. *Acta Ecol. Sin.* **2007**, *27*, 989–996.
42. Du, S.; Liu, G.B. *Ecological Function of Vegetation Restoration on the Loess Plateau*; Science Press: Beijing, China, 2015.
43. Li, G.Q.; Wen, Z.M.; Guo, K.; Du, S. Simulating the effect of climate change on vegetation zone distribution on the Loess Plateau, Northwest China. *Forests* **2015**, *6*, 2092–2108. [CrossRef]
44. Wang, X.M.; Zhang, C.X.; Hasi, E.; Dong, Z.B. Has the tree norths forest shelterbelt program solved the desertification and dust storm problems in arid and semiarid China? *J. Arid Environ.* **2010**, *74*, 13–22. [CrossRef]
45. Feng, X.M.; Fu, B.J.; Piao, S.L.; Wang, S.; Ciais, P.; Zeng, Z.Z.; Lu, Y.H.; Zeng, Y.; Li, Y.; Jiang, X.H.; et al. Revegetation in China's Loess Plateau is approaching sustainable water resource limits. *Nat. Clim. Chang.* **2016**, *6*, 1019–1022. [CrossRef]
46. Pan, Y.; Wang, Y.; Zheng, S.; Huete, A.R.; Shen, M.; Zhang, X.; Huang, J.; He, G.; Yu, L.; Xu, X.; et al. Characteristics of greening along altitudinal gradients on the Qinghai–Tibet Plateau based on time-series Landsat images. *Remote Sens.* **2022**, *14*, 2408. [CrossRef]
47. Xue, J.; Su, B. Significant remote sensing vegetation indices: A review of developments and applications. *J. Sens.* **2017**, *2017*, 1353691. [CrossRef]
48. Bai, Z.G.; Dent, D.L.; Olsson, L.; Schaepman, M.E. Proxy global assessment of land degradation. *Soil Use Manag.* **2008**, *24*, 223–234. [CrossRef]
49. Alcaraz-Segura, D.; Chuvieco, E.; Epstein, H.E.; Kasischke, E.S.; Trishchenko, A. Debating the greening vs. browning of the North American boreal forest: Differences between satellite datasets. *Glob. Chang. Biol.* **2010**, *16*, 760–770. [CrossRef]
50. Xu, X.L. *Spatial Distribution Data Set of Annual Vegetation Index (NDVI) in China*; Data Registration and Publishing System of Resource and Environmental Science Data Center, Chinese Academy of Sciences: Beijing, China, 2018. [CrossRef]
51. Cerasoli, F.; D'Alessandro, P.; Biondi, M. Worldclim 2.1 versus Worldclim 1.4: Climatic niche and grid resolution affect between-version mismatches in habitat suitability models predictions across Europe. *Ecol. Evol.* **2022**, *12*, e8430. [CrossRef]

52. DiCola, V.; Broennimann, O.; Petitpierre, B.; Breiner, F.T.; DAmen, M.; Randin, C.; Engler, R.; Pottier, J.; Pio, D.; Dubuis, A.; et al. ecospat: An R package to support spatial analyses and modeling of species niches and distributions. *Ecograhpy* **2016**, *40*, 774–787. [CrossRef]
53. Schoener, T.W. Nonsynchronous spatial overlap of lizards in patchy habitats. *Ecology* **1970**, *51*, 408–418. [CrossRef]
54. Xin, Z.B.; Xu, J.X.; Zheng, W. Effects of climate change and human activities on vegetation cover change in the Loess Plateau. *Sci. China Earth Sci.* **2007**, *37*, 1504–1514.
55. Zhang, J.Z.; Li, C.Z.; Wang, T. Dynamic change of vegetation coverage on the Loess Plateau and its factors. *Res. Soil Water Conserv.* **2022**, *29*, 224–230, 241.
56. Chang, Q.R.; Xie, B.N. *Vegetation Cover and Its Response to Climate Change in the Loess Plateau in Recent 30 Years*; Science Press: Beijing, China, 2019.
57. Liu, S.; Gong, P. Change of surface cover greenness in China between 2000 and 2010. *Chin. Sci. Bull.* **2012**, *57*, 1423–1434. [CrossRef]
58. Chen, C.; Park, T.; Wang, X.H.; Piao, S.L.; Xu, B.D.; Chaturvedi, R.K.; Fuchs, R.; Brovkin, V.; Ciais, P.; Fensholt, R.; et al. China and India in greening of the world through land-use management. *Nat. Sustain.* **2019**, *2*, 122–129. [CrossRef] [PubMed]
59. Skidmore, A.K.; Franklin, J.; Dawson, T.P.; Pilesjo, P. Geospatial tools address emerging issues in spatial ecology: A review and commentary on the special issue. *Int. J. Geogr. Inf. Sci.* **2011**, *25*, 337–365. [CrossRef]
60. Hay, G.J.; Marceau, D.J.; Bouchard, P.A. A multiscale framework for landscape analysis: Object-specific analysis and upscaling. *Landsc. Ecol.* **2001**, *16*, 471–490. [CrossRef]
61. Guisan, A.; Thuiller, W.; Zimmermann, N.E. (Eds.) 8—Ecological Scales: Issues of Resolution and Extent from Part II—Data Acquisition, Sampling Design, and Spatial Scales. In *Habitat Suitability and Distribution Models with Applications in R*; Cambridge University Press: Cambridge, UK, 2017; pp. 135–150. [CrossRef]
62. Hansen, M.C.; Potapov, P.V.; Moore, R.; Hancher, M.; Turubanova, S.; Tyukavina, A.; Thau, D.; Stehman, S.; Goetz, S.; Loveland, T. High-resolution global maps of 21st-century forest cover change. *Science* **2013**, *342*, 850–853. [CrossRef] [PubMed]
63. Gong, P.; Wang, J.; Yu, L.; Zhao, Y.; Zhao, Y.; Liang, L.; Niu, Z.; Huang, X.; Fu, H.; Liu, S.; et al. Finer resolution observation and monitoring of global land cover: First mapping results with Landsat TM and ETM+ data. *Int. J. Remote Sens.* **2013**, *34*, 2607–2654. [CrossRef]
64. Chen, B.; Xu, B.; Zhu, Z.; Yuan, C.; Suen, H.P.; Guo, J.; Xu, N.; Li, W.; Zhao, Y.; Yang, J.J.S.B. Stable classification with limited sample: Transferring a 30-m resolution sample set collected in 2015 to mapping 10-m resolution global land cover in 2017. *Sci. Bull.* **2019**, *64*, 370–373. [CrossRef]
65. Piao, S.L.; Yin, G.D.; Tan, J.G.; Cheng, L.; Huang, M.T.; Li, Y.; Liu, R.G.; Mao, J.F.; Myneni, R.B.; Peng, S.S.; et al. Detection and attribution of vegetation greening trend in China over the last 30 years. *Glob. Chang. Biol.* **2015**, *21*, 1601–1609. [CrossRef]
66. Tian, F.; Fensholt, R.; Verbesselt, J.; Grogan, K.; Horion, S. Evaluating temporal consistency of long term global NDVI datasets for trend analysis. *Remote Sens. Environ.* **2015**, *163*, 326–340. [CrossRef]
67. Dellinger, A.S.; Essl, F.; Hojsgaard, D.; Kirchheimer, B.; Klatt, S.; Dawson, W.; Pergl, J.; Pysek, P.; Kleunen, M.; Weber, E.; et al. Niche dynamics of alien species do not differ among sexual and apoptotic flowering plants. *New Phytol.* **2016**, *209*, 1313–1323. [CrossRef]